# A Double Closed-Loop Control Method for Quasi-Resonant Converter

CHUN-SEN TANG, HAO SHEN
College of Automation
Chongqing University
No.174, Sha Zheng Street, Chongqing
CHINA
cstang@cqu.edu.cn, 280824599@qq.com

XIAO LV
Chongqing Special Equipment Inspection and Research Institute
No.5 Furongyuan Road Northern New Chongqing
CHINA
395629531@qq.com

*Abstract:* - To achieve the soft-switching condition and stabilize the output voltage of quasi-resonant converters, the paper proposes a double closed-loop control method (DCCM). In the inner loop, soft-switching is guaranteed with the off-time of the switch determined by the zero-crossing signal of the switching voltage. In the outer loop, the output voltage is regulated to be constant against load variations by controlling the on-time of the switch according to the error between the output voltage and the reference voltage. The operation principle and implementation of the proposed method have been investigated in detail on an example BUCK zero-voltage-switching quasi-resonant converter. Both simulation and experiment results have verified the validation of the proposed method.

*Key-Words:* - soft-switching, zero-voltage quasi-resonant converter, double closed-loop control, proportional-integral (PI) controller

## 1 Introduction

In pulse width modulation (PWM) converters, power is processed by interrupting the power flow and regulation is attained by controlling duty cycle. By adding an LC tank, several classes of soft-switching converters, so-called quasi-resonant converters (QRCs), are derived [1]. The sinusoidal voltage waveform generated by the waveform-shaping LC tank creates a zero-voltage condition (soft-switching condition) for the switch to turn on without switching stresses and losses, reducing electromagnetic interference (EMI). Moreover, at soft-switching condition, switching frequency can be increased with high power density.

However, the control principle of the PWM converters can't apply to QRCs directly. QRCs are another family of DC-DC converters, in which the resonant network is used to transfer power as a medium and regulation is usually obtained by controlling switching frequency [2]-[11]. These converters are especially different from PWM converters and resonant converters because of their special circuit features and characteristics [12]. QRCs are regarded as hybrid system between PWM converters and resonant converters.

Soft-switching technology is presented in 1970s, it includes series-paralle1 resonant technology, multiple resonant technology, quasi-resonant technology, ZVS-PWM and ZCS-PWM [13]-[14]. A mathematical expression is provided in [15] to determine the occurrence of soft-switching for a general topology of ZVT converters with auxiliary resonant circuit. This expression can help designer to choose appropriate values for auxiliary resonant branch. A novel soft-switched auxiliary resonant tank is proposed in [16] to provide a zero-voltage condition at turn on for a PWM boost converter in a power factor correction application. A high efficiency converter for switched reluctance motor drives is developed in [17], the power semiconductor device is employed to implement its high-speed PWM switches and the soft-switching control is employed to reduce their switching losses.

The innovation of this paper is utilizing a double closed-loop control method (DCCM) to achieve the soft-switching condition and stabilize the output voltage of quasi-resonant converters. This paper is

organized as follows: in Section 2 the operation principle is described and the steady-mathematical model is built. Section 3 provides the design formulas for resonant parameters and analysis for critical soft-switching conditions. A double closed-loop controller is designed in Section 4. In section 5 and 6, the proposed method is verified by both SIMULINK simulation and experiment results.

## 2 The operation principle and steady-state mathematical model

A zero-voltage quasi-resonant converter is shown in Fig.1, This topology is based on the *BUCK* circuit. The *LC* resonant circuit ($L_r$, $C_r$) is used to shape the voltage wave through switch *S*. The ideal steady state waveform of the circuit is shown in Fig.2. $u_g$ is the control signal of *S*. $u_{cr}$ is the voltage of $C_r$. $i_{Lr}$ is the current of $L_r$. $T_s$ is the switching period, where $t_{on}$ and $t_{off}$ are *on* and *off* durations.

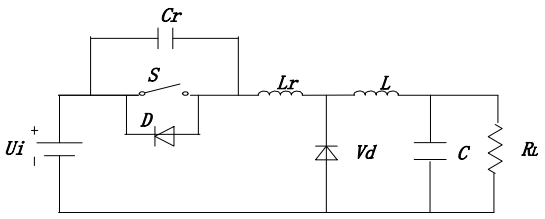


Fig.1 The circuit topology of ZVSQRC

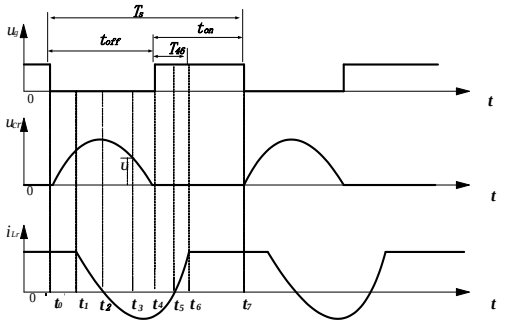


Fig.2 The ideal steady state waveforms of the circuit

To analyze its steady-state circuit behavior, the following assumptions are made.

- $L$ is much larger than $L_r$.
- Output filter $L$-$C$ and the load $R_L$ are treated as a constant current sink $I_o$.
- Semiconductor switches and reactive elements of tank circuit are ideal.

The following variables are defined:

- Resonant angular frequency $\omega_r = 1/\sqrt{L_r C_r}$
- Resonant frequency $f_n = \omega_r / 2\pi$
- Characteristic impendence $Z_n = \sqrt{L_r / C_r}$
- Normalized load $r = R_L / Z_n$

As shown in Fig.2, supposing $t_0$ is the starting time, a steady state switching cycle can be divided into four stages: Charging, Resonant, Recovering, Freewheeling. The steady state mathematical models are shown as follows:

$$\begin{cases} i_{Lr}(t) = I_o \\ u_{cr}(t) = (I_o / C_r)(t\text{-}t_0) \end{cases}, t \in [t_0, t_1] \quad (1)$$

$$\begin{cases} i_{Lr}(t) = I_o \cos\omega_r(t\text{-}t_1) \\ u_{cr}(t) = U_i + Z_n I_o \sin\omega_r(t\text{-}t_1) \end{cases}, t \in [t_1, t_4] \quad (2)$$

$$\begin{cases} i_{Lr}(t) = \dfrac{U_i}{L_r}(t\text{-}t_4) + I_o \cos\omega_r(t_4 - t_1) \\ u_{cr}(t) = 0 \end{cases}, t \in [t_4, t_6] \quad (3)$$

$$\begin{cases} i_{Lr}(t) = I_o \\ u_{cr}(t) = 0 \end{cases}, t \in [t_6, t_7] \quad (4)$$

From the (1), (2), (3), and(4), the duration of four stages can be derived : $T_{01}=U_i C_r / I_o$, $T_{14}=\partial / \omega_r$, $T_{46}= I_o L_r(1+\cos\partial)/U_i$, defining $\partial = \arcsin\{-U_i/(Z_n I_o)\}$.

## 3 Critical soft-switching conditions and resonant parameters design

From the (2), to achieve zero-voltage soft-switching , the input voltage $U_i$ must meet $Z_n I_o \geqslant U_i$. The system is under the critical soft-switching conditions while $Z_n I_o = U_i$. Since $I_o = U_o / R_L$, the voltage conversion ratio $x$ can be derived:

$$x = U_o / U_i = R_L / Z_n \quad (5)$$

$$\partial = \arcsin\{-U_i / (Z_n I_o)\} = 3\pi/2 \quad (6)$$

As shown in Fig.2, the *off* duration can be derived:

$$t_{off} = T_{01} + T_{14} = \frac{2 + 3\pi}{2\omega_r} \quad (7)$$

It is found that $t_{off}$ is a constant under the critical soft-switching conditions, it is only associated with the resonant angular frequency $\omega_r$.

As shown in Fig.2, during $t_{on}$, there is a switching point $t_6$ .

- Switch *S* is turned off after $t_6$, that is $t_{on} \geq T_{46}$,

Assuming $E_i$ is input energy per cycle, $E_o$ is output energy per cycle, thus

$$E_o = U_o I_o T_s \quad (8)$$

$$E_i = U_i\int_{t_0}^{t_1} i_{Lr}dt + U_i\int_{t_1}^{t_4} i_{Lr}dt + U_i\int_{t_4}^{t_6} i_{Lr}dt + U_i(t_{on}-t_{46})I_o \quad (9)$$

From (8) and (9), the $t_{on}$ can be solved by equating $E_i$ and $E_o$

$$t_{on} = \frac{(2+3\pi)x+2}{2\omega_r(1-x)} \quad (11)$$

Defining $\alpha$ is duty cycle of system, so

$$\alpha = \frac{t_{on}}{T_s} = \frac{(2+3\pi)x+2}{4+3\pi} \quad (12)$$

Given the values of $x$, the duty cycle $\alpha$ can be solved by (12). It is found that $\alpha$ have a linear relation with $x$.

From (11) and (12), the relationship between resonant frequency $f_n$ and switch frequency $f_s$ ($f_s$=1/$T_S$) can be derived:

$$f_n == \frac{(4+3\pi)f_s}{4\pi(1-x)} \quad (13)$$

Since resonant inductance $L_r$=$Z_n$/(2π$f_n$) and resonant capacitance $C_r$=1/(2π$f_n Z_n$), from (5) and (13), $L_r$ and $C_r$ can be solved:

$$\begin{cases} L_r = \dfrac{2(1-x)R_L}{(4+3\pi)xf_s} \\ C_r = \dfrac{2(1-x)x}{(4+3\pi)R_L f_s} \end{cases} \quad (14)$$

- Switch $S$ is turned off before $t_6$, that is $t_{on} \le T_{46}$,

As shown in Fig.2, the resonant currant $i_{Lr}$ haven't rises to the output currant $I_o$ when switch $S$ is off during $T_{46}$, as a result, diode $V_d$ can't be off, the system is equivalent to two subsystem as follows:

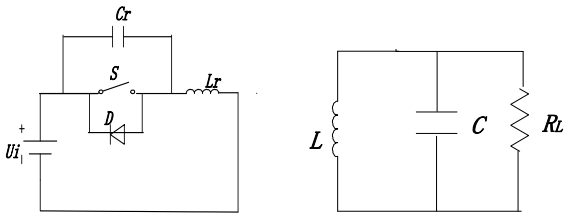


Fig. 3 (a) Free resonant system
(b) Damping system

As shown in Fig.3(a), during $S$ is on, $L_r$ is charged by dc voltage source $U_i$ .when $S$ is off, a resonant circuit was formed ($L_r$,$C_r$ and $U_i$ ). Since the on-time of $S$ is reduced, the energy stored in $L_r$ is decreased, the peak of $u_{cr}$ is reduced gradually until it can't reach zero. As a result, switch $S$ can't be on, the system is instability.

As shown in Fig.3(b), due to the effect without excitation source, the magnetic energy in $L$ and the field energy in $C$ are not disappeared immediately, the energy is gradually consumed by load $R_L$.

From the above, $T_{46}$ is critical on-time:

$$T_{46} = xL_r / R_L \quad (15)$$

Notice that, 0<$x$<1, 0<$T_{46}$ <$L_r$/$R_L$. So the system on-time $t_{on}$ can be derived:

$$t_{on} \ge L_r / R_L \quad (16)$$

# 4 Double closed-loop controller design

To achieve the soft-switching condition and stabilize the output voltage of quasi-resonant converter, on the one hand, the switching voltage $u_{cr}$ must be detected to guarantee the soft-switching by the zero-crossing signal of $u_{cr}$, on the other hand, the output voltage must be detected to be regulated to a constant against load variations by controlling the on-time of the switch according to the error between the output voltage and the reference voltage. A double closed-loop controller was shown in Fig.4. $u_o(t)$ is output voltage, $u_{ref}(t)$ is reference voltage, $u_{cr}(t)$ is switching voltage. From the Fig.4, the error signal can be defined:

$$e(t) = u_{\text{ref}} - u_o(t) \quad (17)$$

Defining $d_{ect}$ zero-crossing detection signals:

$$d_{ect} = \begin{cases} 1 & u_{cr}(t) > 0 \\ 0 & u_{cr}(t) \le 0 \end{cases} \quad (18)$$

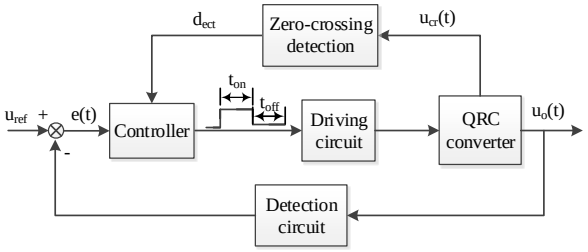


Fig.4 Voltage type double closed-loop feedback controller

As shown in Fig.4, in the inner loop, soft-switching is achieved with the off-time of the switch determined by the zero-crossing signal of the switching voltage. In the outer loop, the output voltage is controlled to be stable by controlling the on-time of the switch according to the error between the output voltage and the reference voltage, the two loops are regulated by one controller. From (7) and (11), $t_{off}$ is a constant with fixed resonant parameters and $t_{on}$ is a variable varied with the voltage-conversion ratios $x$. That is the switching period $T_s$ ($T_s$= $t_{off}$+ $t_{on}$) changes with change of state of system. Thus the control method is a pulse frequency modulation (PFM) method, as shown in Fig.5.

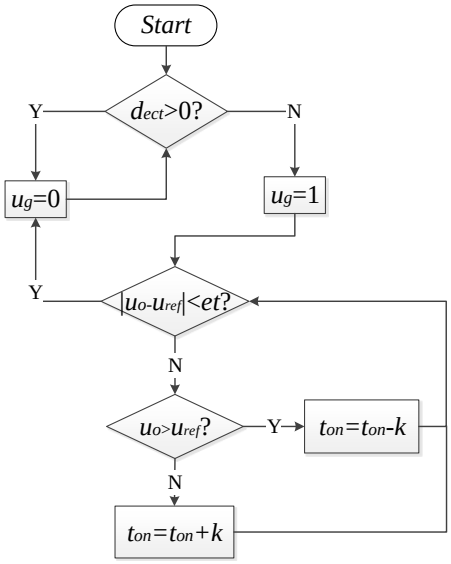


Fig. 5 Control flow chart

*Start* is enabling signal. *k* is the control step , on-time of switching *S* is regulated by *k*. *et* is the error signals, the ripple wave of the output voltage is regulated by *et*.

# 5 Simulation and experiment

## 5.1 Simulation model

To analyze the performance of the controller as shown in Fig.4, a simulation model is built as shown in Fig.5. System parameters are shown in table 1.

Assuming stable switching frequency $f_s$=100kHz, as shown in Tab.1, given the values of $U_i$, $U_{ref}$, $f_s$ and $R_L$, the values of $x$, $L_r$ and $C_r$ can be solved from (5) and (14).

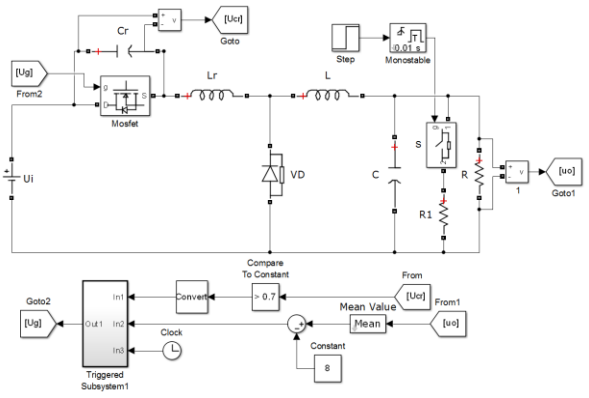


Fig. 6 The simulation model of double closed-loop control system

Tab.1 System parameter selection table

| parameters | values |
|---|---|
| Input voltage $U_i$（V） | 12 |
| Reference voltage $U_{ref}$（V） | 8 |
| Resonant inductive$L_r$（μH） | 7.5 |
| Resonant capacitive $Cr$(nF) | 33 |
| Filter inductive $L$(mH) | 0.38 |
| Filter capacitive $C$(mF) | 0.26 |
| Load1 $R_L$(Ω) | 10 |
| Load2 $R_L$(Ω) | 20 |

## 5.2 Soft-switching characteristics analysis

As shown in Tab.1, two different loads are chosen to analyze the characteristics of soft-switching. Also a critical reference voltage ($U_{ref}$=2V) is chosen to observe the nonlinear-phenomena. The simulation time is set to 0.1s, the simulation algorithm adopts *ode23tb*, and the maximum simulation step is set up to 1e-5. The results of simulation are shown in Fig.7 (a)~(f).

As can be seen from Fig.7(a), it's about 5ms that the system enters a stable state under the control method and its overshoot is very small, illustrating the system has a great starting performance. When at 10ms, the load is switched from 10Ω to 20Ω, the balance of system is broken, about 5ms, the values of output voltage stabilize at 8V again. It can be found that the recovery time of system is extremely fast.

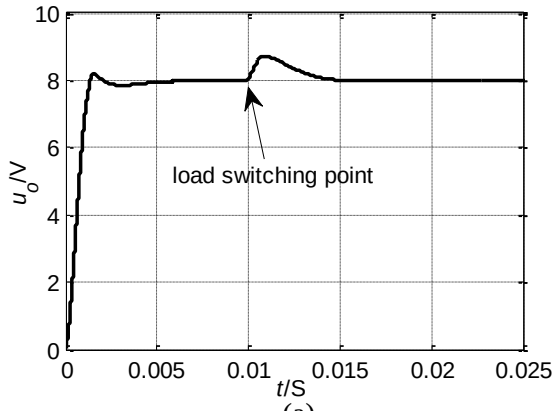


(a)

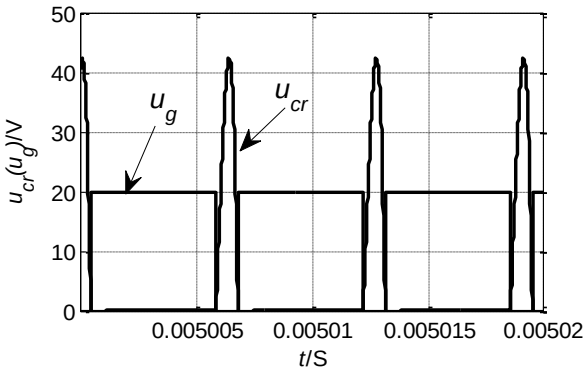


(b)

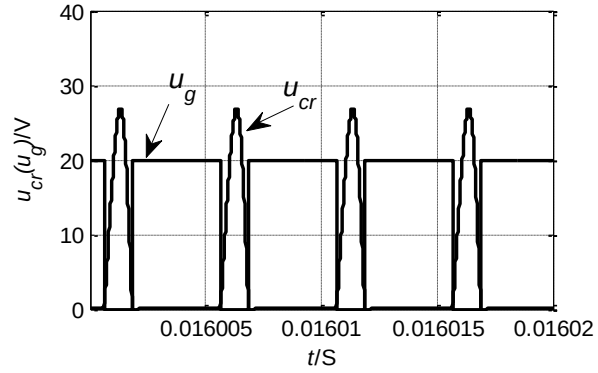


(c)

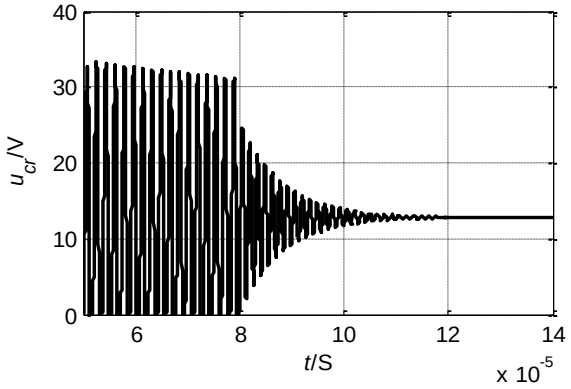


(d)

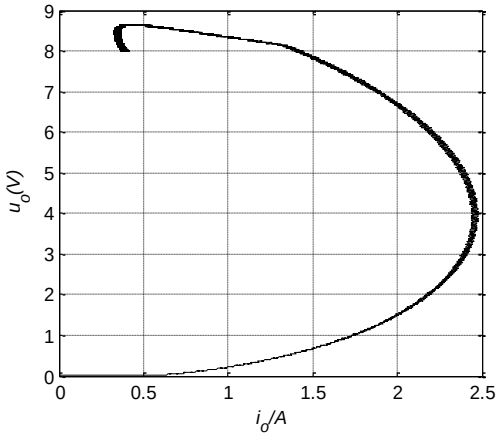


(e)

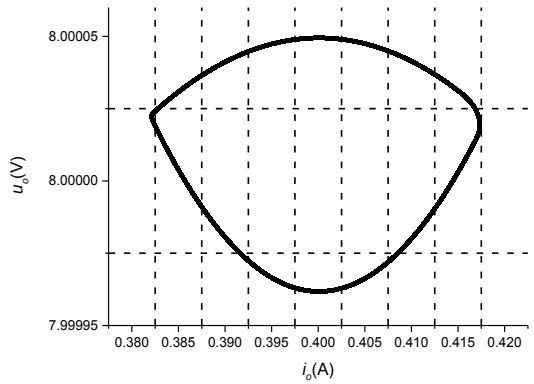


(f)

Fig.7 The system simulation results (a) output voltage waveform, (b) driving signal and resonant voltage waveforms with $R_L$=10Ω, (c) driving signal and resonant voltage waveforms with $R_L$=20Ω, (d) resonant voltage waveforms with $u_{ref}$ =2V, (e) phase plane of the converter, (f) steady behavior presents limit cycle

Fig.7(b) and (c) shows, under the different load conditions ($R_L$=10Ω or $R_L$=20Ω), switch *S* achieves the soft-switching condition successfully. And the peak of switch voltage is cut down when changing heavy load to light load.

As shown in Fig.7(d), during the time 0~0.08 ms, the peak of switch voltage $u_{cr}$ gradually lowers caused by the reduction of the switch on-time. At 0.08 ms, $u_{cr}$ can't reach zero, as a result, switch *S* can't be off anymore, the system is divided into two subsystems as shown in Fig.3(a) and (b).Because of the resistance, $u_{cr}$ eventually oscillation damping to the input voltage $U_i$.

Fig.7(e) and (f) shows the phase plane of the converter, it has limit cycle to which trajectories starting from other initial conditions appear to be attracted.

In general, not only soft-switching condition is achieved but also output voltage is stabilized under the control method proposed this paper. However, as shown in Fig.7(d) , there is a dead-on-time in this family of converter, thus, to avoid the unstable state, the lower limit of on-time should be set to an appropriate value from (16).

## 5.3 Experimental verifications

A quasi-resonant buck converter with a resonant frequency of 100 KHz is built to verify the double closed-loop control method presented in section 4. The circuit diagram is shown in Fig.1 and component values are shown in Tab.1. MOSFET semiconductors IRF460 are selected as the switches of the converters. A STC12C5612 microcontroller is used to generate the control signal for switch.

It can be found from Fig.8 that the switch *S* is on at zero-voltage condition and the output voltage $u_o$ is regulated to 8V steadily. The delay time in Fig.8 is caused by zero-crossing detection *LM311*.

Fig.9 presents experimental waveforms of the output voltage and switching frequency at load switching. It is observed from the figure that the DCCM has the ability to regulate the output voltage to set-point with the settling time of 4.6 ms and about 5% overshoot when load switch. What's more, the switching frequency is changed from $f_s$=100KHz to $f_s$=75KHz. The overshoot can be reduced by appropriately decreasing control step *k*.

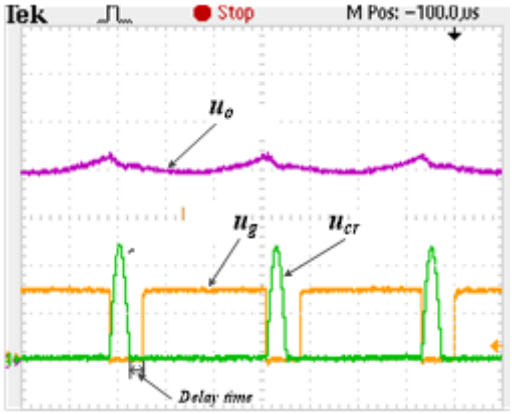


Fig.8 The driving signal $u_g$(5V/div), switching voltage $u_{cr}$(10V/div), output voltage $u_o$(2V/div) .

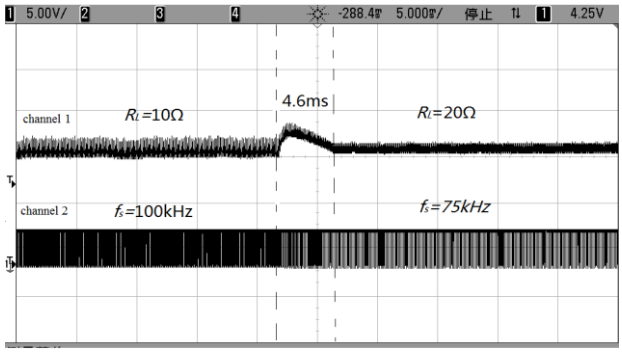


Fig.9 The output voltage and switching frequency waveforms of load switching (channel 1 is output voltage and channel 2 is switch frequency)

The result of simulation and experiment show that the DCCM has good stability, accuracy, rapidity and it has strong ability to resist load switching.

## 6 Conclusion

In this paper, a double closed-loop control method (DCCM) is proposed to achieve the soft-switching condition and stabilize the output voltage of quasi-resonant converter. Moreover, the critical soft-switching condition is analyzed in detail to derive the critical on-time and the design formulas of resonant parameters ($L_r$ and $C_r$) for ZVS-QRC. The results are verified by both SIMULINK simulation and practical experiments.

## Acknowledgement

The authors would like to express their sincere thanks to the anonymous reviewers for their invaluable suggestions and comments to improve this paper. This work is supported by the National Natural Science Foundation of China under Grant 51207173 and the Fundamental Research Funds of ChongQing under Grant cstc2013jcyjA0235.

*References:*

[1] M. Jabbari. Unified Analysis of Switched-Resonator Converters, *Power Electronics, IEEE Transactions on*, Vol.26, No.5, 2011, pp. 1364-1376.

[2] D. Maksimovic and Slobodan. Cuk, Constant-frequency control of quasi-resonant converters, *Power Electronics, IEEE Transactions on*, Vol.6, No.1, 1991, pp. 141-150.

[3] M. B. Borage, K. Nagesh, M. S. VBhatia and S Tiwari. Characteristics and Design of an Asymmetrical Duty-Cycle-Controlled LCL-T Resonant Converter, *Power Electronics, IEEE Transactions on*, Vol.24, No.10, 2009, pp.2268-2275.

[4] M. Foster, C. P. Gould, A. R. Gilbert, D. J. Stone, C M. A. Bingham. Analysis of CLL Voltage-Output Resonant Converters Using Describing Functions, *Power Electronics, IEEE Transactions on*, Vol.23, No.4, 2008, pp. 1772-1781.

[5] Dianbo Fu, F. C. Lee, Yang Qiu and F. Wang. A Novel High-Power-Density Three-Level LCC Resonant Converter With Constant-Power-Factor-Control for Charging Applications, *Power Electronics, IEEE Transactions on*, Vol.23, No.5, 2008, pp. 2411-2420.

[6] Dianbo Fu, Ya Liu, F. C. Lee, Ming Xu. A Novel Driving Scheme for Synchronous Rectifiers in LLC Resonant Converters, *Power Electronics, IEEE Transactions on*, Vol.24, No.5, 2011, pp. 1321-1329.

[7] Daocheng Huang, Dianbo Fu, F. C. Lee. High switching frequency, high efficiency CLL resonant converter with synchronous rectifier, in *Proc. IEEE Energy Covers. Congr. Expo (ECCE)*, 2009, pp. 804-809.

[8] G. Ivensky, I. Zeltser, A. Kats and S. Ben-Yaakov. Reducing IGBT losses in ZCS series resonant converters, *Power Electronics, IEEE Transactions on*, Vol.46, No.1, 1999, pp. 67-74.

[9] M. Jabbari and H. Farzanehfard. Family of soft-switching resonant DC-DC converters, *IET Power Electron*, Vol.2, No.2, 2009, pp. 113-124.

[10] M. Jabbari. Resonant inverting-buck converter, *IET Power Electron*, Vol.3, No.4, 2009, pp. 571-577.

[11] M. Jabbari and H. Farzanehfard. New Resonant Step-Down/Up Converters, *Power Electronics*,

*IEEE Transactions on*, Vol.26, No.1, 2010, pp. 249-256.

[12] S. Sharifi, M . Jabbari, H. Farzanehfard, F B Darani. A resonant LLC boost converter, *Applied Electronics (AE), 2012 International Conference on,* pp. 257-260

[13] S. Mosavi and G Moschopoulos. A New ZCS-PWM Full-Bridge Dc-Dc Converter with Simple Auxiliary CircUits, *Power Electronics, IEEE Transactions on,* Vol.29, No.3, 2013, pp.1321-1330.

[14] M. Vuksic, S. M. Bero and L. Vuksic. The Multiresonant Converter Steady-State Analysis Based on Dominant Resonant Process, *Power Electronics, IEEE Transactions on,* Vol.26, No.5, 2011, pp.1452-1468.

[15] J. L. Russi, V. F. Montagner, M. L. Da Silva Martins and H L Hey. A Simple Approach to Detect ZVT and Determine Its Time of Occurrence for PWM Converters, *Industrial Electronics, IEEE Transactions on,* Vol.60, No.7, 2013, pp. 2576-585.

[16] I. Aksoy, H. Bodur and F. A. Bakan. A New ZVT-ZCT-PWM DC-DC Converter, *Power Electronics, IEEE Transactions on,* Vol.25, No.8, 2010, pp.2093-2105.

[17] K. H. Chao. A novel soft-switching converter for switched reluctance motor drives, *WSEAS Transactions on Circuits and Systems,*Vol.8, No.5, 2009, pp.411-421.